Original Article

# Evaluating the predictive value of optical coherence tomography angiography metrics and central corneal thickness among glaucoma suspect patients: a comparative cross-sectional study

Fathy Mohamed Abo Elftouh Elsalhy [1] , Sarah Abbas Alshamarti [2] , Saif Abbas Alshamarti [2] , Abdelrahman Ahmed Ali Khattab [1] , Mahmoud Mohammed Ahmed Ali Khalil [1] , Mahmoud Fawzy Zaky Morsy [1] , Ahmad Mohammad Salah Eldeen Abdul Hay [1] , Ezzat Nabil Abbas Ibrahim [1] , Ahmed Mohammed Madinah Alkady [1] , Mahmoud Ahmed Shafeek [1], Bassem Ismail Khalil Gomaa [1] and Mohamed Sayed Taha Abouzeid [3]

[1] *Faculty of Medicine, Al-Azhar University, Cairo, Egypt*

[2] *Faculty of Medicine, University of Al-Qadisiyah, Iraq*

[3] *Faculty of Medicine, Beni Suef university, Egypt*

**ABSTRACT**

**Background:** Glaucoma suspects (GS) exhibit risk factors such as elevated intraocular pressure (IOP), suspicious optic disc or retinal nerve fiber layer (RNFL) findings, or a positive family history, yet their risk of progression varies widely. Optical coherence tomography angiography (OCTA) and central corneal thickness (CCT) have emerged as important markers for detecting early structural and microvascular changes in GS patients. We aimed to estimate the predictive value of OCTA-derived metrics and CCT, and to assess their correlations in GS individuals.

**Methods:** This comparative cross-sectional study included eyes from GS patients and eyes from age- and sex-matched healthy individuals as a comparison group. All participants underwent a detailed medical history and comprehensive ophthalmologic examination. Investigations included visual field perimetry; optical coherence tomography (OCT) to assess structural optic nerve head parameters, RNFL thickness, and ganglion cell layer (GCL) thickness; OCTA to measure papillary vascular density (PVD) and radial peripapillary capillary density (RPC); and non-contact specular microscopy to determine CCT.

**Results:** The GS group had a mean age of 36.9 years, with 52.4% male (n = 11). GS eyes showed significantly larger CDR values, reduced rim area, thinner RNFL and GCL, and lower CCT compared with healthy eyes (all $P < 0.05$). Mean RPC, quadrant-specific RPC values, and mean PVD were significantly reduced in GS individuals (all $P < 0.05$). CCT showed significant correlations with all vascular metrics and structural parameters (all $P < 0.05$), except disc area ($P > 0.05$). In univariate logistic regression all variables were associated with GS status. After multivariate adjustment, only CCT ≤ 506 μm remained an independent predictor. Receiver operating characteristic curve analysis showed good diagnostic performance for CCT (area under the curve [AUC] = 0.757) and mean RPC (AUC = 0.820) in identifying GS eyes.

**Conclusions:** Patients with GS revealed significantly lower structural parameters and vascular metrics compared with the healthy group, and only thin CCT remained an independent predictor of GS status. Both CCT and mean RPC demonstrated good diagnostic performance for identifying GS eyes.

**KEYWORDS**

glaucomas, radial peripapillary capillary vessel density, corneal thickness measurement, peripapillary retinal nerve fiber layer thickness, intraocular pressures, optic nerves, optical coherence tomography, area under curves, specificity and sensitivity

**Correspondence:** Abdelrahman Ahmed Ali Khattab, Faculty of medicine, Al-Azhar University, Cairo, Egypt. Email: abdulrahmankhattab88@gmail.com, ORCID iD: https://orcid.org/0000-0003-4632-8506.

**How to cite this article:** Elsalhy FMAE, Alshamarti SA, Alshamarti SA, Khattab AAA, Khalil MMAA, Morsy MFZ, Abdul Hay AMSE, Ibrahim ENA, Alkady AMM, Shafeek MA, Gomaa BIK, Abouzeid MST. Evaluating the predictive value of optical coherence tomography angiography metrics and central corneal thickness among glaucoma suspect patients: a comparative cross-sectional study. Med Hypothesis Discov Innov Ophthalmol. 2025 Winter; 14(4): 183-193. https://doi.org/10.51329/mehdiophthal1531

Received: 02 November 2025; Accepted: 08 December 2025

## INTRODUCTION

Glaucoma is a leading cause of irreversible blindness worldwide and is characterized by progressive retinal ganglion cell loss, optic nerve head (ONH) damage, and thinning of the retinal nerve fiber layer (RNFL) [1] Although the pathophysiology of glaucoma remains incompletely understood, vascular mechanisms are thought to contribute to its pathogenesis [2]. The vascular theory proposes that insufficient ocular perfusion—whether due to elevated intraocular pressure (IOP) or other factors that compromise blood flow—may lead to glaucomatous optic neuropathy. Reduced blood flow can promote oxidative stress through increased production of reactive oxygen species and upregulation of inflammatory mediators [1].

Glaucoma suspects (GS) are individuals who exhibit clinical features or risk factors that increase the likelihood of developing glaucoma, such as elevated IOP, suspicious appearance of optic disc or RNFL, visual field defects that do not meet diagnostic criteria for glaucoma, or a positive family history. The rate at which GS individuals progress to glaucoma varies widely and depends on the specific risk factors and clinical findings present [3].

Optical coherence tomography angiography (OCTA) enables rapid, non-invasive, in vivo, qualitative and quantitative assessment of the retinal and ONH microvasculature by detecting blood flow-related motion contrast through repeated structural B-scans. It has been widely used to characterize microvascular compromise in glaucoma, evidencing good diagnostic capability [4]. Central corneal thickness (CCT) also represents a key parameter in the evaluation of GS patients. Both RNFL defects and reduced CCT are important measures in risk stratification for GS individuals [5].

We aimed to evaluate the predictive value of OCTA-derived vascular metrics and CCT, as well as to explore their correlations, in GS individuals.

## METHODS

In this comparative cross-sectional study, eligible participants were consecutively recruited from the ophthalmology outpatient clinics of Al-Azhar University Hospitals in Cairo, Egypt between December 2023 and June 2024. The study adhered to the ethical principles of the Declaration of Helsinki and received approval from the Research Ethics Committee of the Faculty of Medicine, Al-Azhar University. Written informed consent was obtained from all participants prior to enrollment.

We compared eyes of GS individuals with eyes from age- and sex-matched ocularly healthy participants who served as the comparison group. Inclusion criteria for the GS group comprised normal or elevated IOP (≥ 22 mmHg) on at least two separate assessment sessions (≥2 standard deviations above the mean IOP), optic disc morphology clinically suggestive of glaucomatous damage with visual field findings that did not meet diagnostic criteria for glaucoma, RNFL abnormalities detected by optical coherence tomography (OCT), and/or a positive family history of glaucoma in the absence of manifest disease [6]. Participants were excluded if they had glaucomatous visual field defects, corneal scarring, keratoconus, a history of refractive surgery, coexisting retinal pathology, non-glaucomatous optic neuropathy, uveitis, high myopia (≥ –6.00 D), or uncontrolled diabetes mellitus.

Before enrollment and prior to obtaining informed consent, all participants underwent a comprehensive evaluation that included a detailed medical and ophthalmic history. Information was recorded regarding family history of glaucoma, lifestyle factors (e.g., smoking: yes vs. no), systemic conditions (diabetes: yes vs. no; hypertension; and low blood pressure, with frequencies of normal vs. low blood pressure documented), history of ocular trauma or prior ocular surgery, previous and current medications, and history of spectacle use.

The ophthalmic examination included assessment of best-corrected visual acuity (BCVA) using a Snellen chart (auto chart projector CP-670; Nidek Co., Ltd., Gamagori, Japan), with values converted to logarithm of the minimum angle of resolution (logMAR) for statistical analysis. IOP was measured by applanation tonometry (AT900®, Haag–Streit, Koeniz, Switzerland). Anterior segment evaluation and gonioscopy were performed with slit-lamp biomicroscopy (Haag–Streit Photo-Slit Lamp BX 900; Haag–Streit AG, Koeniz, Switzerland). Fundus examination using a +90 D lens (Volk Optical, Inc., Mentor, OH, USA) was conducted to assess posterior segment and optic disc morphology.

Imaging was performed using a swept-source OCT system (SS-OCT; DRI OCT Triton, Topcon Corporation, Tokyo, Japan) to evaluate ONH parameters including disc area, rim area, cup area, cup-to-disc area ratio (CDR), vertical CDR (VCDR), horizontal CDR (HCDR), and cup volume, as well as RNFL and GCL thickness. The TOPCON OCT device's built-in analysis software references a normative database to determine cut-off values based on the

statistical distribution of measurements in healthy eyes. Only participants with OCT classifications of 'normal' or 'borderline' were included in this study [7].

OCTA imaging was performed using an SS-OCT Angio system (DRI OCT Triton; Topcon Inc., Tokyo, Japan) to measure papillary vascular density (PVD) within ONH layer and radial peripapillary capillary (RPC) vascular density. Each scan was centered on the optic disc using a 4.5 × 4.5 mm acquisition area. Three predefined slabs—retina, RPC, and choroid—were analyzed. The device's built-in software automatically generated quantitative vascular density values. Vessel density is the proportion of the peripapillary region occupied by both large vessels and microvasculature. It measures superior, nasal, inferior, and temporal quadrants, along with the superior-hemi and inferior-hemi peripapillary regions [8] (Figure 1).

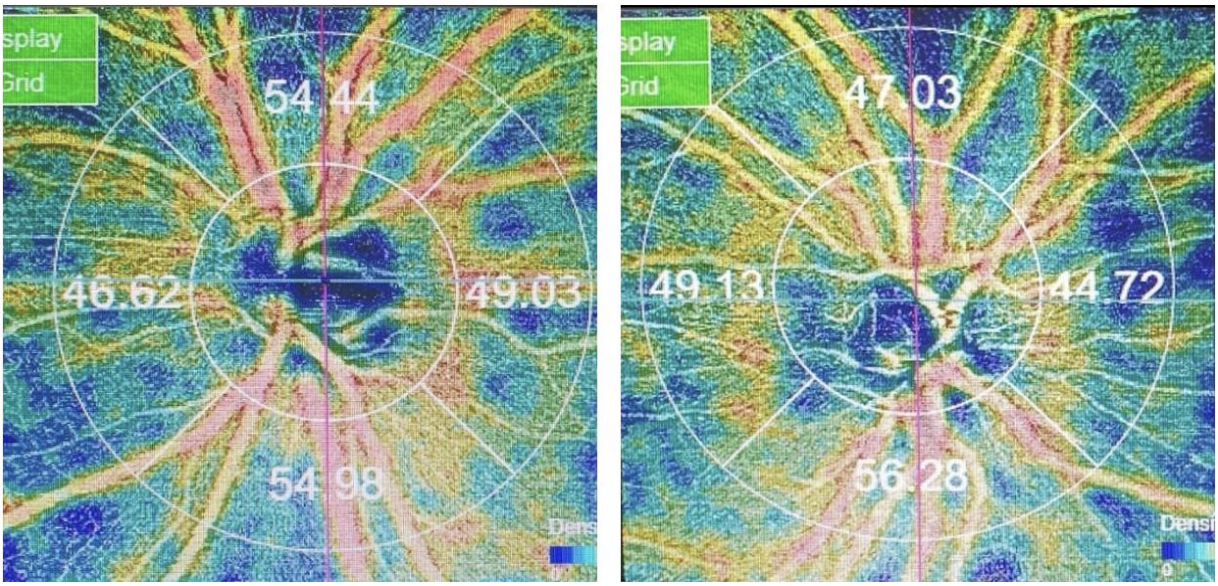


**Figure 1. Swept-source optical coherence tomography angiography (SS-OCTA) of the optic nerve head and peripapillary region: SS-OCTA (DRI OCT Triton, Topcon Inc., Tokyo, Japan) showing papillary vascular density (PVD) and radial peripapillary capillary (RPC) vascular density in the right and left eyes of a study participant. The 4.5 × 4.5 mm peripapillary scan displays sector-wise vessel density measurements generated by the device's built-in analysis software.**


**Figure 2. Central corneal thickness measurements obtained using a non-contact specular microscope (SP-1P, Topcon Corporation, Tokyo, Japan) in the right and left eyes of the same participant shown in Figure 1. The device provides fully automated image capture and endothelial cell analysis. Abbreviations: CCT, central corneal thickness; CD, cell density; CV, coefficient of variation; HEX, hexagonality; N, number of endothelial cells counted.**

CCT was measured using a non-contact specular microscope (SP-1P, Topcon Corporation, Tokyo, Japan), which acquires images through a fully automated capture process and operates within a measurement range of 400–750 μm. The device analyzes reflections generated at interfaces of differing refractive indices as the imaging beam traverses the cornea [9] (Figure 2).

Visual field perimetry was performed using the Humphrey Field Analyzer (Humphrey Field Analyzer HFA: Carl Zeiss Meditec Inc., Dublin, CA, USA) to exclude participants with glaucomatous visual field defects.

Statistical analyses were performed using IBM SPSS Statistics for Windows, Version 25.0 (IBM Corp., Armonk, NY, USA). Data distribution was assessed using the Shapiro–Wilk test. Normally distributed variables were reported as mean and standard deviation (SD) and compared using the independent *t*-test, non-normally distributed variables were presented as median and interquartile range (IQR) and analyzed using the Mann–Whitney U test. Categorical variables were compared using the Chi-square test or Fisher's exact test when expected cell counts were <5. Correlations between continuous variables were examined using Spearman's coefficient, with correlation strength interpreted as strong (≥0.70), moderate (0.40–0.69), or weak (<0.40). Variables that differed significantly between groups—namely family history of glaucoma, smoking status, and low blood pressure—were treated as potential confounders. To adjust for their influence, these factors were included as covariates in the multivariate logistic regression model assessing predictors of GS status, ensuring that estimated associations for CCT, RPC, and PVD reflected independent effects rather than confounding influences. Univariate logistic regression was first performed for all relevant demographic, clinical, and imaging variables. Variables with $P < 0.20$ in univariate analyses and those considered clinically relevant were entered into the initial multivariate logistic regression model to determine independent predictors of GS status (binary outcome: 0 = healthy comparison group, 1 = GS), which was then refined using the backward: Wald method to derive the most parsimonious set of independent predictors. For categorical predictors, reference categories were defined as follows: non-smokers for smoking; CCT > 506 μm for CCT ≤ 506 μm; CDR ≤ 0.4 for CDR > 0.4; mean RPC > 48.2 μm for mean RPC ≤ 48.2 μm; mean PVD > 47.09 μm for mean PVD ≤ 47.09 μm; total GCL thickness > 68 μm for total GCL thickness ≤ 68 μm; mean RNFL thickness > 109 μm for mean RNFL thickness ≤ 109 μm; rim area > 1.56 $mm^2$ for rim area ≤ 1.56 $mm^2$; HCDR ≤ 0.52 for HCDR > 0.52; and VCDR ≤ 0.52 for VCDR > 0.52. The logistic model was constructed using the backward: Wald elimination method, and results are presented as odds ratios (OR) with 95% confidence intervals (CIs) and corresponding *P*-values for both univariate and multivariate models. For continuous outcomes (e.g., CCT and mean RPC), multivariate linear regression models were fitted using the Enter method. Prior to model entry, multicollinearity was assessed using variance inflation factor (VIF) and tolerance values; all VIF values were < 5, indicating no significant multicollinearity and acceptable independence among predictors. Standardized coefficients (β) were used to evaluate the relative contribution of each predictor, while unstandardized coefficients (B) quantified effect sizes. Regression analyses were conducted on the combined dataset (GS and comparison eyes), with the "group" variable adjusted for as a covariate. Receiver operating characteristic (ROC) curve analysis was performed to evaluate the diagnostic performance of CCT, mean RPC, inferior RPC, and mean PVD in identifying GS eyes. Optimal cutoff points were determined using Youden's Index (sensitivity + specificity − 1). These four markers were selected based on clinical relevance, prior literature linking them to early glaucomatous structural or microvascular alterations, and their statistical significance or near-significance in the present study's analyses, even though CCT emerged as the only independent predictor in multivariate modeling. All statistical tests were two-tailed. A *P*-value < 0.05 was considered statistically significant and *P*-value < 0.01 highly significant.

## RESULTS

We included 42 eyes from 21 GS individuals and 42 eyes from 21 age- and sex-matched ocularly healthy participants who served as the comparison group. Sociodemographic characteristics of the participants are summarized in Table 1. Mean (SD) age of individuals in the GS group was 36.9 (16.4) years, and slightly more than half were male (n = 11, 52.4%). A positive family history of glaucoma was reported in 57.1% (n = 12) of GS participants. Only 9.5% (n = 2) had diabetes mellitus, whereas smoking and low blood pressure were present in 47.6% (n = 10) and 61.9% (n = 13) of them, respectively. Two groups were comparable in terms of mean age, sex ratio, or diabetes status (all $P > 0.05$), while the family history of glaucoma, smoking, and low blood pressure differed significantly between groups (all $P < 0.05$) (Table 1). These variables were not central to the primary study objectives though.

Table 2 summarizes IOP, BCVA, CCT, and OCT-derived parameters. Mean IOP and BCVA did not differ significantly between GS and comparison eyes (both $P < 0.05$). GS eyes showed significantly larger OCT-derived CDR

values (all $P < 0.05$). Rim area was significantly reduced in GS eyes ($P < 0.001$), whereas disc area showed a non-significant trend toward reduction ($P > 0.05$). Cup volume was significantly larger in GS eyes compared with the comparison group ($P < 0.001$). Mean total GCL and mean RNFL thicknesses were both significantly lower in GS eyes (both $P < 0.05$). Consistent with this pattern, CCT was significantly lower among GS participants ($P < 0.001$). Compared with comparison eyes, GS eyes exhibited significant reductions in mean RPC value, quadrant-specific RPC values, and mean PVD (all $P < 0.05$) (Table 2).

The correlation analysis in the GS group focused on CCT, mean RPC, and mean PVD, as these variables showed significant inter-group differences and represent key indicators of ocular structural and vascular status. Additional correlations were evaluated but were non-significant and therefore not reported. Correlation analyses for CCT, inferior and mean RPC, and mean PVD with ocular parameters are presented in Table 3. CCT evidenced a strong positive correlation with mean RPC (r = + 0.72, $P < 0.001$); a strong negative correlation with HCDR (r = −0.93, $P < 0.001$); moderate positive correlations with inferior RPC (r = + 0.48, $P = 0.001$), mean PVD (r = +0.65, $P < 0.001$), total GCL thickness (r = +0.44, $P < 0.05$), mean RNFL thickness (r = +0.60, $P < 0.001$), and rim area (r = +0.51, $P = 0.001$); and a moderate negative correlation with CDR (r = −0.68, $P < 0.001$), VCDR (r = −0.67, $P < 0.001$), and cup volume (r = −0.63, $P < 0.001$), yet no significant correlation with disc area (r = +0.04, $P > 0.05$) (Table 3).

Regression findings are summarized in Tables 4 and 5. In the multivariate linear model predicting CCT (Table 4), mean RNFL thickness was a significant positive predictor ($P < 0.05$), with each 1-μm increase in RNFL thickness associated with a corresponding 1.14-μm increase in CCT. Higher CDR and VCDR values were significantly associated with reduced CCT (both $P < 0.05$), indicating that greater optic disc cupping is linked to thinner corneas. Rim area evidenced a borderline positive association ($P = 0.052$), whereas mean RPC did not significantly predict CCT ($P > 0.05$) (Table 4).

**Table 1. Sociodemographic characteristics of study groups**

| Variables | Comparison group (n = 21) | Glaucoma suspect (n. = 21) | *P*-value |
|---|---|---|---|
| **Age (y), Mean ± SD (Range)** | 28.9 ± 9.7 (19 to 62) | 36.9 ± 16.4 (19 to 72) | [a] 0.061 |
| **Sex (Male / Female), n (%)** | 7 (33.3) / 14 (66.7) | 11 (52.4) / 10 (47.6) | [b] 0.212 |
| **FH of glaucoma (No / Yes), n (%)** | 16 (76.2) / 5 (23.8) | 9 (42.9) / 12 (57.1) | [b] **0.028** |
| **Smoking (No / Yes), n (%)** | 18 (85.7) / 3 (14.3) | 11 (52.4) / 10 (47.6) | [b] **0.019** |
| **DM (No / Yes), n (%)** | 21 (100.0) / 0 (0.0) | 19 (90.5) / 2 (9.5) | [b] 0.147 |
| **BP (Normal / Low), n (%)** | 15 (71.4) / 6 (28.6) | 8 (38.1) / 13 (61.9) | [b] **0.030** |

**Abbreviations: n, number of participants; y, years; SD, standard deviation; FH, family history; %, percentage; DM, diabetes mellitus; BP, blood pressure. Note: *P*-values < 0.05 are shown in bold; [a] *P*-value was derived from the independent *t*-test; [b] *P*-value was derived from the chi-square test.**

**Table 2. Values of ocular parameters in study groups**

| Variables | Comparison group (n = 42) | Glaucoma suspect (n. = 42) | *P*-value |
|---|---|---|---|
| **BCVA (logMAR), Mean ± SD (Range)** | 0.05 ± 0.07 (0 to 0.2) | 0.07 ± 0.09 (0 to 0.4) | [a] 0.097 |
| **IOP (mmHg), Mean ± SD (Range)** | 18.3 ± 3.1 (11 to 22) | 19.3 ± 3.0 (14 to 29) | [b] 0.119 |
| **CDR (ratio), Mean ± SD (Range)** | 0.4 ± 0.2 (0.1 to 0.7) | 0.6 ± 0.1 (0.3 to 0.8) | [b] **< 0.001** |
| **HCDR (ratio), Mean ± SD (Range)** | 0.6 ± 0.2 (0.2 to 0.8) | 0.7 ± 0.1 (0.4 to 0.9) | [b] **0.026** |
| **VCDR (ratio), Mean ± SD (Range)** | 0.5 ± 0.2 (0.1 to 0.8) | 0.6 ± 0.1 (0.3 to 0.8) | [b] **< 0.001** |
| **CCT (μm), Mean ± SD (Range)** | 529.3 ± 50.7 (431 to 629) | 485.2 ± 36.6 (428 to 615) | [b] **< 0.001** |
| **Rim area ($mm^2$), Mean ± SD (Range)** | 2.6 ± 1.2 (0.9 to 5.4) | 1.5 ± 0.9 (0.6 to 5.0) | [b] **< 0.001** |
| **Disc area ($mm^2$), Mean ± SD (Range)** | 3.2 ± 1.3 (1.6 to 6.3) | 2.7 ± 1.0 (1.26 to 6.01) | [b] 0.054 |
| **Cup volume ($mm^3$), Mean ± SD (Range)** | 0.1 ± 0.1 (0 to 0.5) | 0.4 ± 0.2 (0.1 to 1.17) | [b] **< 0.001** |
| **Total GCLT (μm), Mean ± SD (Range)** | 65.7 ± 5.5 (51 to 73) | 62.5 ± 5.2 (51 to 70) | [b] **0.007** |
| **Mean RNFLT (μm), Mean ± SD (Range)** | 109.3 ± 11.3 (62.8 to 123.8) | 100.1 ± 13.4 (62.8 to 128.5) | [b] **0.001** |
| **Inferior RPC (μm), Mean ± SD (Range)** | 52.4 ± 2.2 (45.9 to 56.7) | 48.9 ± 3.3 (40.1 to 55.4) | [b] **< 0.001** |
| **Superior RPC (μm), Mean ± SD (Range)** | 51.4 ± 2.4 (45.5 to 54.8) | 49.1 ± 3.1 (39.2 to 55.7) | [b] **< 0.001** |
| **Nasal RPC (μm), Mean ± SD (Range)** | 44.4 ±3.3 (38.3 to 50.7) | 42.7 ± 3.3 (36.4 to 50.8) | [b] **0.019** |
| **Temporal RPC (μm), Mean ± SD (Range)** | 47.0 ± 2.4 (40.4 to 50.2) | 45.6 ± 3.0 (38.2 to 51.0) | [b] **0.020** |
| **Mean RPC (μm), Mean ± SD (Range)** | 48.8 ±1.7 (44.8 to 52.2) | 46.6 ± 2.0 (40.5 to 51.8) | [b] **< 0.001** |
| **Mean PVD (μm), Mean ± SD (Range)** | 47.8 ± 2.9 (41 to 52.6) | 46.2 ± 3.0 (39.1 to 51.0) | [b] **0.018** |

**Abbreviations: n, number of eyes; BCVA, best-corrected visual acuity; logMAR, logarithm of the minimum angle of resolution; SD, standard deviation; IOP, intraocular pressure; mmHg, millimeter of mercury; CDR, cup-to-disc ratio; HCDR, horizontal cup-to-disc ratio; VCDR, vertical cup-to-disc ratio; CCT, central corneal thickness; μm, micrometer; GCLT, ganglion cell layer thickness; RNFLT, retinal nerve fiber layer thickness; RPC, radial peripapillary capillary vascular density; PVD, peripapillary vascular density. Note: *P*-values < 0.05 are shown in bold; [a] *P*-value was derived from the Mann–Whitney test; [b] *P*-value was derived from the independent *t*-test.**

**Table 3. Correlation of CCT, Inferior RPC, mean RPC vascular density, and mean PVD with other ocular parameters in GS individuals**

| Variables | CCT | Inferior RPC | Mean RPC | Mean PVD |
|---|---|---|---|---|
| CCT | – | ***P*-value = 0.001**<br>**r-value=+ 0.48** | ***P*-value < 0.001**<br>**r-value=+ 0.72** | ***P*-value < 0.001**<br>**r-value=+ 0.65** |
| Inferior RPC | ***P*-value = 0.001**<br>**r-value=+ 0.48** | – | ***P*-value < 0.001**<br>**r-value=+ 0.80** | ***P*-value < 0.001**<br>**r-value=+ 0.66** |
| Mean RPC | ***P*-value < 0.001**<br>**r-value=+ 0.72** | ***P*-value < 0.001**<br>**r-value=+ 0.80** | – | ***P*-value < 0.001**<br>**r-value=+ 0.74** |
| Mean PVD | ***P*-value < 0.001**<br>**r-value=+ 0.65** | ***P*-value < 0.001**<br>**r-value=+ 0.66** | ***P*-value < 0.001**<br>**r-value=+ 0.74** | – |
| CDR | ***P*-value < 0.001**<br>**r-value=- 0.68** | ***P*-value = 0.014**<br>**r-value=- 0.38** | ***P*-value < 0.001**<br>**r-value=- 0.54** | ***P*-value = 0.031**<br>**r-value=- 0.33** |
| Total GCLT | ***P*-value = 0.003**<br>**r-value=+ 0.44** | ***P*-value = 0.001**<br>**r-value=+ 0.51** | ***P*-value < 0.001**<br>**r-value=+ 0.64** | ***P*-value = 0.001**<br>**r-value=+ 0.49** |
| Mean RNFLT | ***P*-value < 0.001**<br>**r-value=+ 0.60** | ***P*-value = 0.001**<br>**r-value=+ 0.51** | ***P*-value < 0.001**<br>**r-value=+ 0.65** | ***P*-value = 0.002**<br>**r-value=+ 0.46** |
| Rim area | ***P*-value = 0.001**<br>**r-value=+ 0.51** | ***P*-value = 0.018**<br>**r-value=+ 0.36** | ***P*-value = 0.003**<br>**r-value=+ 0.45** | ***P*-value = 0.004**<br>**r-value=+ 0.44** |
| Disc area | *P*-value = 0.797<br>r-value=+ 0.04 | *P*-value = 0.659<br>r-value=+ 0.07 | *P*-value = 0.793<br>r-value=+ 0.04 | *P*-value = 0.715<br>r-value=- 0.06 |
| HCDR | ***P*-value < 0.001**<br>**r-value=- 0.93** | ***P*-value < 0.001**<br>**r-value=- 0.55** | ***P*-value < 0.001**<br>**r-value=- 0.76** | ***P*-value < 0.001**<br>**r-value=- 0.65** |
| VCDR | ***P*-value < 0.001**<br>**r-value=- 0.67** | ***P*-value = 0.020**<br>**r-value=- 0.36** | ***P*-value = 0.001**<br>**r-value=- 0.49** | ***P*-value = 0.001**<br>**r-value=- 0.50** |
| Cup Volume | ***P*-value < 0.001**<br>**r-value=- 0.63** | ***P*-value = 0.002**<br>**r-value=- 0.47** | ***P*-value < 0.001**<br>**r-value=- 0.61** | ***P*-value < 0.001**<br>**r-value=- 0.58** |

**Abbreviations: GS, glaucoma suspect; CCT, central corneal thickness; RPC, radial peripapillary capillary vascular density; PVD, peripapillary vascular density; CDR, cup-to-disc ratio; GCLT, ganglion cell layer thickness; RNFLT, retinal nerve fiber layer thickness; HCDR, horizontal cup-to-disc ratio; VCDR, vertical cup-to-disc ratio. Note: *P*-values < 0.05 are shown in bold; correlation coefficients (r) and corresponding *P*-values were calculated using Spearman's rank correlation.**

**Table 4. Multiple linear regression analysis of predictors of CCT**

| Variables | B (Unstandardized Coefficients) | SE | Beta (Standardized Coefficients) | t | *P*-value | 95% CI for B |
|---|---|---|---|---|---|---|
| **Constant** | 515.57 | 94.28 | — | 5.47 | **< 0.001** | 331.80 to 699.37 |
| **CDR** | - 93.54 | 33.00 | - 0.29 | - 2.84 | **0.008** | -158.20 to -28.88 |
| **Mean RNFLT** | 1.14 | 0.45 | 0.42 | 2.53 | **0.016** | 0.260 to 2.02 |
| **Rim area** | 8.07 | 4.02 | 0.21 | 2.01 | 0.052 | 0.19 to 15.94 |
| **VCDR** | - 87.29 | 34.97 | - 0.27 | - 2.50 | **0.017** | -155.83 to -18.75 |
| **Mean RPC** | 1.74 | 1.83 | 0.10 | 0.95 | 0.348 | -1.84 to 5.32 |

**Abbreviations: CCT, central corneal thickness; SE, standard error; CI, confidence interval; CDR, cup-to-disc ratio; RNFLT, retinal nerve fiber layer thickness; VCDR, vertical cup-to-disc ratio; RPC, radial peripapillary capillary vascular density. Note: P-values < 0.05 are shown in bold. Model summary: $R^2 = 0.612$; adjusted $R^2 = 0.558$; $F(5, 36) = 11.36$; $P < 0.001$. Method: Enter (all predictors entered simultaneously). Dependent variable: CCT.**

**Table 5. Multiple linear regression analysis of predictors of mean RPC**

| Variables | B (Unstandardized Coefficients) | SE | Beta (Standardized Coefficients) | t | *P*-value | 95% CI for B |
|---|---|---|---|---|---|---|
| **Constant** | 23.84 | 8.66 | — | 2.75 | **0.009** | 6.26 to 41.41 |
| **CCT** | 0.03 | 0.01 | 0.56 | 2.24 | **0.032** | 0.003 to 0.06 |
| **Total GCLT** | 0.10 | 0.10 | 0.25 | 0.98 | 0.335 | -0.11 to 0.30 |
| **Mean RNFLT** | 0.004 | 0.05 | 0.03 | 0.09 | 0.928 | -0.09 to 0.10 |
| **Rim area** | 0.49 | 0.39 | 0.23 | 1.25 | 0.218 | -0.30 to 1.29 |
| **Disc area** | - 0.35 | 0.30 | - 0.16 | - 1.17 | 0.250 | -0.95 to 0.25 |
| **VCDR** | 2.47 | 3.29 | 0.14 | 0.75 | 0.458 | -4.21 to 9.14 |

**Abbreviations: RPC, radial peripapillary capillary vascular density; SE, standard error; CI, confidence interval; CCT, central corneal thickness; GCL, ganglion cell layer thickness; RNFLT, retinal nerve fiber layer thickness; VCDR, vertical cup-to-disc ratio. Note: *P*-values < 0.05 are shown in bold; Model summary: $R^2 = 0.545$; adjusted $R^2 = 0.467$; $F(6, 35) = 6.988$; $P < 0.001$. Method: Enter (all predictors entered simultaneously). Dependent variable: mean RPC.**

**Table 6. Univariate and multivariate logistic regression analyses of factors associated with glaucoma-suspect status**

| Variables | Univariate OR (95% CI) | *P*-value | Multivariate OR (95% CI) | *P*-value |
|---|---|---|---|---|
| **FH of glaucoma** | 4.27 (1.13 to 16.05) | 0.032 | - | - |
| **Smoking** | 5.46 (1.23 to 24.26) | 0.026 | - | - |
| **Low BP (mmHg)** | 4.06 (1.12 to 14.80) | 0.034 | - | - |
| **CDR > 0.4** | 57.00 (14.85 to 218.73) | < 0.001 | - | - |
| **CCT ≤ 506 (μm)** | 23.75 (6.95 to 81.15) | < 0.001 | **18.44 (2.61 to 130.53)** | **0.004** |
| **Mean RPC ≤ 48.2 (μm)** | 16.00 (5.44 to 47.04) | < 0.001 | - | - |
| **Mean PVD ≤ 47.09 (μm)** | 6.40 (2.46 to 16.66) | < 0.001 | - | - |
| **Total GCLT ≤ 68 (μm)** | 11.11 (2.35 to 52.56) | 0.002 | - | - |
| **Mean RNFLT ≤ 109 (μm)** | 5.58 (2.19 to 14.22) | < 0.001 | 5.86 (0.87 to 39.40) | 0.069 |
| **Rim area ≤ 1.56 (mm²)** | 34.83 (9.81 to 123.64) | < 0.001 | - | - |
| **HCDR > 0.52** | 7.85 (2.37 to 25.95) | 0.001 | - | - |
| **VCDR > 0.52** | 15.44 (4.63 to 51.45) | < 0.001 | - | - |

**Abbreviations: OR, odds ratio; CI, confidence interval; BP, blood pressure; CDR, cup-to-disc ratio; CCT, central corneal thickness; RPC, radial peripapillary capillary vascular density; PVD, papillary vascular density; GCLT, ganglion cell layer thickness; RNFLT, retinal nerve fiber layer thickness; HCDR, horizontal cup-to-disc ratio; VCDR, vertical cup-to-disc ratio; GS, glaucoma-suspect. Note: *P*-values < 0.05 are shown in bold; Reference category for all ORs is the healthy comparison group. Univariate logistic regression was conducted for all candidate variables, with those showing P < 0.20 and clinically relevant factors entered into the multivariate model. Independent predictors of GS status (0 = healthy, 1 = GS) were identified using the Backward: Wald method. ORs with 95% CIs are reported. Reference categories were: non-smokers (smoking); CCT > 506 μm; CDR ≤ 0.4; mean RPC > 48.2 μm; mean PVD > 47.09 μm; total GCLT > 68 μm; mean RNFLT > 109 μm; rim area > 1.56 mm²; HCDR ≤ 0.52; and VCDR ≤ 0.52.**

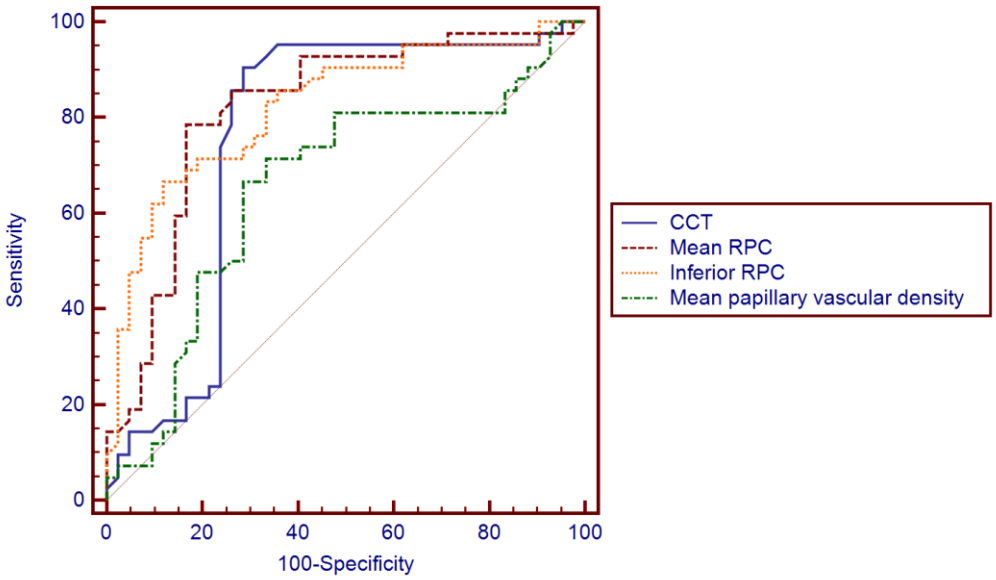


**Figure 3. Receiver operating characteristic (ROC) curves showing the diagnostic performance of central corneal thickness (CCT), mean radial peripapillary capillary vascular density (mean RPC), inferior RPC, and mean papillary vascular density in detecting glaucoma-suspect eyes. The curves illustrate the area under the curve (AUC), sensitivity, specificity, positive predictive value (PPV), and negative predictive value (NPV) for each parameter.**

In the model predicting mean RPC (Table 5), CCT emerged as the only significant independent predictor. A 1 μm increase in CCT was associated with a 0.03% increase in mean RPC ($P < 0.05$), reflecting a modest yet statistically significant positive relationship. Other structural parameters were not significantly associated with mean RPC (all $P > 0.05$) (Table 5). Overall, these regression models suggest that CCT is influenced by optic nerve structural characteristics, particularly RNFL thickness and degree of optic disc cupping. Conversely, RPC appears to depend primarily on CCT, supporting an interrelationship between early microvascular and structural changes in GS eyes.

Univariate and multivariate logistic regression analyses are presented in Table 6. Several parameters—including family history of glaucoma, smoking, low blood pressure, increased CDR values, reduced CCT, reduced total GCL thickness, lower mean RNFL thickness, lower rim area, and lower mean RPC and PVD—were significantly associated with GS status in univariate analysis (all $P < 0.05$) (Table 6). After multivariate adjustment, CCT ≤ 506 μm remained

the sole independent predictor (OR = 18.44, 95 % CI: 2.61–130.53; $P < 0.05$). Mean RNFL ≤ 109 μm showed a trend toward significance (OR = 5.86, 95 % CI: 0.87–39.40, $P = 0.069$) (Table 6).

ROC analyses for CCT, mean RPC, inferior RPC, and mean PVD are presented in Figure 3. CCT predicted GS at a cutoff ≤ 506 μm (area under the curve [AUC] = 0.757), evidencing high sensitivity (90.5%), specificity of 71.4%, a positive predictive value (PPV) of 76.0%, and a negative predictive value (NPV) of 88.2%. Mean RPC, with a cutoff ≤ 48.2 μm, exhibited strong overall discriminative ability (AUC = 0.820), yielding 78.6% sensitivity, 83.3% specificity, a PPV of 82.5%, and an NPV of 79.5%. Inferior RPC predicted GS at a cutoff ≤ 50.3 μm (AUC = 0.823), providing the highest specificity (88.1%), along with 66.7% sensitivity, 84.8% PPV, and 72.5% NPV. In contrast, mean PVD evidenced comparatively weaker diagnostic performance, identifying GS at a cutoff ≤ 47.09 μm (AUC = 0.654) with 66.7% sensitivity, 71.4% specificity, a PPV of 70.0%, and an NPV of 68.2%. Clinically, these findings suggest that CCT serves as a sensitive early screening marker (minimizing false negatives), inferior RPC functions as a highly specific confirmatory parameter, and mean RPC offers the most balanced overall diagnostic performance. By comparison, mean PVD shows limited utility for early GS detection. The ROC curves in Figure 3 visually illustrate these differences, with curves farther from the diagonal line of equality indicating greater diagnostic accuracy.

## DISCUSSION

The objectives of the present study were to evaluate the predictive value of OCTA-derived vascular metrics and CCT, and to assess their correlations among GS individuals. Regarding demographic and clinical characteristics, the proportion of smokers was significantly higher in the GS group compared with the comparison group, consistent with findings by Nishida et al., who reported that smoking is associated with reduced vessel density and may contribute to glaucoma development [10]. Additionally, there were significantly more individuals with low blood pressure in the GS group. This concords with a previous report showing that hypotension correlates with reduction of ocular perfusion pressure, predisposing the optic nerve to ischemia [11].

In this study, mean RPC and quadrant-specific RPC values were significantly lower in GS individuals than in the comparison group. These findings align with Liu et al. [12], who documented significantly reduced mean global RPC in GS (42.78 [2.28] μm) compared with controls (45.7 [2.31] μm). Similarly, inferior and nasal RPC values were significantly reduced in GS (43.38 [4.61] μm and 33.08 [7.35] μm, respectively) compared with controls (47.40 [3.59] μm and 38.91 [4.60] μm, respectively) [12].

The mean PVD was significantly lower in GS individuals (46.2 [3.0] μm) compared with the comparison group (47.8 [2.9] μm). Akil et al. [13], using SS-OCTA, found significantly lower mean PVD in pre-perimetric glaucoma (PPG) (83.86% [5]) relative to normal eyes (91.7% [2.7]), further supporting the role of early microvascular compromise in glaucoma [13].

We observed significantly thinner mean CCT in GS eyes (485.2 [36.6] μm) compared with the comparison group (529.3 [50.7] μm). This finding is consistent with Mehta et al., who reported reduced ganglion cell inner plexiform layer (GCIPL) complex and RNFL thickness in PPG, accompanied by significantly thinner CCT (544 [8.8] μm) compared with healthy eyes (551.4 [30] μm) [14]. Belbase et al. similarly reported mean CCT values of 498.55 (35.08) μm for POAG, 519.50 (25.92) μm for GS, and 529.5 (18.49) μm for normal participants. In their study, the mean CCT value in POAG differed significantly from both GS and normal eyes, whereas CCT differences between GS and normal controls were not significant [15]. Oba et al. [16] reported lower median CCT in GS (529.1 μm) compared with normal eyes (537.2 μm), though this was not statistically significant [16].

Structural optic nerve parameters differed significantly between study groups. The mean CDR was significantly higher in GS (0.6 [0.1]) than in the comparison group (0.4 [0.2]). HCDR and VCDR were likewise greater in GS (0.7 [0.1] and 0.6 [0.1], respectively) compared with controls (0.6 [0.2] and 0.5 [0.2]). Rim area was significantly reduced in GS (1.5 [0.9] $mm^2$) relative to controls (2.6 [1.2] $mm^2$), whereas disc area was comparable (2.7 [1.0] vs. 3.2 [1.3] $mm^2$). Cup volume was significantly larger in GS (0.4 [0.2] $mm^3$) compared with the comparison group (0.1 [0.1] $mm^3$). These observations concur with Hong et al., who reported a larger median CDR in GS (0.6) compared with normal eyes (0.4) [17], and with Akil et al., who observed increased CDR in PPG (0.58 [0.12]) versus controls (0.3 [0.1]) [13]. Chen et al. also noted significantly reduced mean rim area (1.11 [0.14] $mm^2$ vs. 1.33 [0.19] $mm^2$) and increased CDR (0.66 [0.10] vs. 0.40 [0.17]) in GS compared with controls [18]. Belbase et al. similarly reported larger CDR values in GS (0.62 [0.62]) and POAG (0.71 [0.07]) compared with normal eyes (0.24 [0.76]) [15]. Rolle et al. found significantly larger VCDR in PPG eyes (0.71 [0.14]) than in controls (0.54 [0.13]), with comparable disc area between groups [19].

A significantly lower total GCL thickness in GS cases (62.5 [5.2] μm) compared with the comparison group (65.7 [5.5] μm) was observed, consistent with Rolle et al., who reported significantly lower average GCL thickness in GS (86.56 [8.57]

μm) and POAG (79.54 [9.37] μm) compared with normal eyes (98.18 [5.37] μm) [19]. Mean RNFL thickness was significantly reduced in GS (100.1 [13.4] μm) compared with the comparison group (109.3 [11.3] μm). Chen et al. documented decreased RNFL thickness in GS (88.7 [9.0] μm) compared with healthy eyes (95.4 [11.8] μm) [18]. Kamalipour et al. similarly documented decreased global RNFL thickness in PPG eyes (90.1 μm) compared with healthy eyes (99.9 μm), with consistent reductions across quadrants [20]. Hong et al. also reported reduced RNFL thickness in GS (88.2 [11.0] μm) compared with controls (92.2 [10.6] μm) [17].

We identified significant positive correlations between CCT and mean RPC, inferior RPC, mean PVD, total GCL, mean RNFL thickness, and rim area, whereas CCT was negatively correlated with CDR, HCDR, and VCDRs, as well as cup volume. These findings reinforce that thinner CCT is associated with glaucomatous optic neuropathy, manifesting as increased cupping and reduced rim area, and that structural alterations correlate with microvascular compromise, as reflected by RNFL, RPC, and PVD reductions. Lotfy et al. [5] similarly reported significant positive correlations between CCT and total, superior, and inferior RPC density, with stronger correlation in eyes exhibiting borderline RNFL thickness [5]. Kollia et al. [21] showed a significant positive correlation between RPC density and RNFL thickness in ocular hypertension, suggesting that greater CCT may be linked to increased RNFL thickness [21]. Mammo et al. [22] also observed that RPC density loss corresponded to RNFL thinning and rim changes, with RPC density correlating strongly with RNFL thickness and visual field performance. The authors suggested that RPC density assessment may serve as a valuable adjunctive tool in the evaluation of glaucomatous optic neuropathy [22]. Gunvant et al. [23] reported significant negative correlations between CCT and cup volume or depth in GS eyes, but not with cup area or shape [23].

To evaluate the predictive role of CCT, RPC vessel density, and PVD, ROC analysis showed that CCT ≤ 506 μm predicted GS with an AUC of 0.757, sensitivity of 90.5%, and specificity of 71.4%. Mean RPC ≤ 48.2 μm predicted GS with an AUC of 0.820, sensitivity of 78.6%, and specificity of 83.3%. Inferior RPC ≤ 50.3 μm yielded the highest AUC (0.823), with sensitivity of 66.7% and specificity of 88.1%. Mean PVD ≤ 47.09 μm showed weaker performance (AUC 0.654), with sensitivity of 66.7% and specificity of 71.4%. Lotfy et al. found total RPC density had an AUC of 0.858 at a cutoff ≤ 51.4, with sensitivity of 72.7% and specificity of 81.2% [5]. Akil et al. reported AUCs of 0.956 and 0.756 for peripapillary area vessel density in distinguishing POAG or PPG from normal eyes [13]. Chung et al. observed AUCs of 0.830 and 0.807 for whole-disc and peripapillary vessel density in differentiating controls from total glaucoma group, with moderate diagnostic ability in early disease (AUCs: 0.754 and 0.726, respectively) [24].

OCTA shows considerable promise in detecting retinal and peripapillary microvascular alterations that may reflect early glaucomatous damage. Nevertheless, the relatively small sample size represents a limitation of our study. Larger, longitudinal studies are needed to clarify how decreases in vascular density interact with established risk factors to influence optic disc morphology and ganglion cell integrity in glaucoma.

## CONCLUSIONS

Patients with GS exhibited significantly lower mean OCTA-derived vascular metrics compared with ocularly healthy individuals. CCT showed positive correlations with mean RPC, inferior RPC, mean PVD, total GCL thickness, mean RNFL thickness, and rim area, while showing negative correlations with cup volume and OCT-derived CDR values. CCT ≤ 506 μm was the only variable that remained significantly associated with GS in multivariate logistic regression analysis. Regarding diagnostic performance, CCT appears to be a sensitive early screening marker, inferior RPC functions as a highly specific confirmatory parameter, and mean RPC provides the most balanced overall accuracy, whereas mean PVD shows limited value for early GS detection. Larger longitudinal studies are needed to further elucidate how vascular density loss interacts with established risk factors to influence optic disc structure and ganglion cell integrity in glaucoma.

## ETHICAL DECLARATIONS

**Ethical approval:** The study adhered to the ethical principles of the Declaration of Helsinki and received approval from the Research Ethics Committee of the Faculty of Medicine, Al-Azhar University. Written informed consent was obtained from all participants prior to enrollment.

**Conflict of interest:** None.

## FUNDING

**None.**

## ACKNOWLEDGMENTS

**None.**

## REFERENCES


1. Dutta A, Thulasidas M, Sasidharan A, Pradeep B, Rajesh Prabu V. Comparison of peripapillary capillary plexus using optical coherence tomography angiography and retinal nerve fibre layer analysis using spectral domain optical coherence tomography in glaucoma patients, glaucoma suspects, and healthy subjects. Indian J Ophthalmol. 2022 Dec;70(12):4146-4151. doi: 10.4103/ijo.IJO_1456_22. PMID: 36453303; PMCID: PMC9940553.
2. El-Nimri NW, Manalastas PIC, Zangwill LM, Proudfoot JA, Bowd C, Hou H, Moghimi S, Penteado RC, Rezapour J, Ekici E, Shoji T, Ghahari E, Yarmohammadi A, Weinreb RN. Superficial and Deep Macula Vessel Density in Healthy, Glaucoma Suspect, and Glaucoma Eyes. J Glaucoma. 2021 Jun 1;30(6):e276-e284. doi: 10.1097/IJG.0000000000001860. PMID: 33899812; PMCID: PMC8169636.
3. Park HL, Shin DY, Jeon SJ, Kim YC, Jung Y, Kim EK, Shin HY, Jung KI, Choi JA, Lee NY, Hong SW, Park CK. Predicting the development of normal tension glaucoma and related risk factors in normal tension glaucoma suspects. Sci Rep. 2021 Aug 17;11(1):16697. doi: 10.1038/s41598-021-95984-7. PMID: 34404847; PMCID: PMC8371169.
4. Bunod R, Lubrano M, Pirovano A, Chotard G, Brasnu E, Berlemont S, Labbé A, Augstburger E, Baudouin C. A Deep Learning System Using Optical Coherence Tomography Angiography to Detect Glaucoma and Anterior Ischemic Optic Neuropathy. J Clin Med. 2023 Jan 7;12(2):507. doi: 10.3390/jcm12020507. PMID: 36675435; PMCID: PMC9865592.
5. Lotfy A, Mattout HK, Fouda SM, Hemeda S. Correlation between radial peripapillary vascular density and reduced central corneal thickness in glaucoma suspect patients. BMC Ophthalmol. 2022 Oct 31;22(1):414. doi: 10.1186/s12886-022-02628-z. PMID: 36316681; PMCID: PMC9620628.
6. Ahmad SS. Glaucoma suspects: A practical approach. Taiwan J Ophthalmol. 2018 Apr-Jun;8(2):74-81. doi: 10.4103/tjo.tjo_106_17. PMID: 30038885; PMCID: PMC6055310.
7. Chaglasian M, Fingeret M, Davey PG, Huang WC, Leung D, Ng E, Reisman CA. The development of a reference database with the Topcon 3D OCT-1 Maestro. Clin Ophthalmol. 2018 May 7;12:849-857. doi: 10.2147/OPTH.S155229. PMID: 29765199; PMCID: PMC5944450.
8. Li C, Tan L, Xu X, Chen S, Huang C. Changes of Optic Disc and Macular Vessel Perfusion Density in Primary Angle Closure Glaucoma: A Quantitative Study Using Optical Coherence Tomography Angiograph. Ophthalmic Res. 2023;66(1):1245-1253. doi: 10.1159/000533874. Epub 2023 Aug 30. PMID: 37647877; PMCID: PMC10614527.
9. Almubrad TM, Osuagwu UL, Alabbadi I, Ogbuehi KC. Comparison of the precision of the Topcon SP-3000P specular microscope and an ultrasound pachymeter. Clin Ophthalmol. 2011;5:871-6. doi: 10.2147/OPTH.S21247. Epub 2011 Jun 24. PMID: 21760714; PMCID: PMC3133003.
10. Nishida T, Weinreb RN, Tansuebchueasai N, Wu JH, Meller L, Mahmoudinezhad G, Gunasegaran G, Adelpour M, Moghimi S. Smoking Intensity is Associated With Progressive Optic Nerve Head Vessel Density Loss in Glaucoma. J Glaucoma. 2024 Jun 1;33(6):394-399. doi: 10.1097/IJG.0000000000002410. Epub 2024 Apr 23. PMID: 38647412.
11. De Moraes CG, Cioffi GA, Weinreb RN, Liebmann JM. New Recommendations for the Treatment of Systemic Hypertension and their Potential Implications for Glaucoma Management. J Glaucoma. 2018 Jul;27(7):567-571. doi: 10.1097/IJG.0000000000000981. PMID: 29750712; PMCID: PMC6028320.
12. Liu L, Lin Y, Xie X, Peng J, Huang C, Ma D, Zhang M. The diagnostic ability of peripapillary vessel density in primary open-angle glaucoma suspects. Photodiagnosis Photodyn Ther. 2024 Oct;49:104271. doi: 10.1016/j.pdpdt.2024.104271. Epub 2024 Jul 25. PMID: 39025396.
13. Akil H, Huang AS, Francis BA, Sadda SR, Chopra V. Retinal vessel density from optical coherence tomography angiography to differentiate early glaucoma, pre-perimetric glaucoma and normal eyes. PLoS One. 2017 Feb 2;12(2):e0170476. doi: 10.1371/journal.pone.0170476. PMID: 28152070; PMCID: PMC5289421.
14. Mehta B, Ranjan S, Sharma V, Singh N, Raghav N, Dholakia A, Bhargava R, Reddy PLS, Bargujar P. The Discriminatory Ability of Ganglion Cell Inner Plexiform Layer Complex Thickness in Patients with Preperimetric Glaucoma. J Curr Ophthalmol. 2024 Mar 29;35(3):231-237. doi: 10.4103/joco.joco_124_23. PMID: 38681693; PMCID: PMC11047817.

15. Belbase U, Maharjan IM, Subedi A. Optical Coherence Tomography Angiography Vessel Density in Healthy, Glaucoma Suspect, and Glaucoma Eyes. J Curr Ophthalmol. 2024 Oct 16;36(1):31-36. doi: 10.4103/joco.joco_270_23. PMID: 39553317; PMCID: PMC11567607.
16. Oba T, Solmaz N, Onder F. Peripapillary and Macular Vascular Density in Patients With Preperimetric and Early Primary Open Angle Glaucoma. J Glaucoma. 2022 Sep 1;31(9):724-733. doi: 10.1097/IJG.0000000000002069. Epub 2022 Jun 21. PMID: 36044326.
17. Hong KL, Burkemper B, Urrea AL, Chang BR, Lee JC, LeTran VH, Chu Z, Zhou X, Xu BY, Wong BJ, Song BJ, Jiang X, Wang RK, Varma R, Richter GM. Hemiretinal Asymmetry in Peripapillary Vessel Density in Healthy, Glaucoma Suspect, and Glaucoma Eyes. Am J Ophthalmol. 2021 Oct;230:156-165. doi: 10.1016/j.ajo.2021.05.019. Epub 2021 Jun 5. PMID: 34102157; PMCID: PMC8599609.
18. Chen CL, Zhang A, Bojikian KD, Wen JC, Zhang Q, Xin C, Mudumbai RC, Johnstone MA, Chen PP, Wang RK. Peripapillary Retinal Nerve Fiber Layer Vascular Microcirculation in Glaucoma Using Optical Coherence Tomography-Based Microangiography. Invest Ophthalmol Vis Sci. 2016 Jul 1;57(9):OCT475-85. doi: 10.1167/iovs.15-18909. PMID: 27442341; PMCID: PMC4968914.
19. Rolle T, Dallorto L, Tavassoli M, Nuzzi R. Diagnostic Ability and Discriminant Values of OCT-Angiography Parameters in Early Glaucoma Diagnosis. Ophthalmic Res. 2019;61(3):143-152. doi: 10.1159/000489457. Epub 2018 Jun 28. PMID: 29953994.
20. Kamalipour A, Moghimi S, Jacoba CM, Yarmohammadi A, Yeh K, Proudfoot JA, Hou H, Nishida T, David RC, Rezapour J, El-Nimri N, Weinreb RN. Measurements of OCT Angiography Complement OCT for Diagnosing Early Primary Open-Angle Glaucoma. Ophthalmol Glaucoma. 2022 May-Jun;5(3):262-274. doi: 10.1016/j.ogla.2021.09.012. Epub 2021 Oct 9. PMID: 34634501; PMCID: PMC9405474.
21. Kollia E, Patsea E, Georgalas I, Brouzas D, Papaconstantinou D. Correlation Between Central Corneal Thickness and Radial Peripapillary Capillary Density, in Patients With Ocular Hypertension. Cureus. 2021 Aug 12;13(8):e17138. doi: 10.7759/cureus.17138. PMID: 34408962; PMCID: PMC8362868.
22. Mammo Z, Heisler M, Balaratnasingam C, Lee S, Yu DY, Mackenzie P, Schendel S, Merkur A, Kirker A, Albiani D, Navajas E, Beg MF, Morgan W, Sarunic MV. Quantitative Optical Coherence Tomography Angiography of Radial Peripapillary Capillaries in Glaucoma, Glaucoma Suspect, and Normal Eyes. Am J Ophthalmol. 2016 Oct;170:41-49. doi: 10.1016/j.ajo.2016.07.015. Epub 2016 Jul 25. PMID: 27470061.
23. Gunvant P, Porsia L, Watkins RJ, Bayliss-Brown H, Broadway DC. Relationships between central corneal thickness and optic disc topography in eyes with glaucoma, suspicion of glaucoma, or ocular hypertension. Clin Ophthalmol. 2008 Sep;2(3):591-9. doi: 10.2147/opth.s2814. PMID: 19668759; PMCID: PMC2694003.
24. Chung JK, Hwang YH, Wi JM, Kim M, Jung JJ. Glaucoma Diagnostic Ability of the Optical Coherence Tomography Angiography Vessel Density Parameters. Curr Eye Res. 2017 Nov;42(11):1458-1467. doi: 10.1080/02713683.2017.1337157. Epub 2017 Sep 14. PMID: 28910159.